# Natamycin interferes with ergosterol-dependent lipid phases in model membranes

Vibeke Akkerman [a,1], Holger A. Scheidt [b,1], Peter Reinholdt [c,1], Mohammad Bashawat [d], Maria Szomek [a], Max Lehmann [e], Pablo Wessig [e], Douglas F. Covey [f,g], Jacob Kongsted [c], Peter Müller [d], Daniel Wüstner [a,*]

[a] Department of Biochemistry and Molecular Biology, University of Southern Denmark, DK-5230, Odense M, Denmark
[b] Institute for Medical Physics and Biophysics, Leipzig University, Härtelstr. 16-18, D-04107, Leipzig, Germany
[c] Department of Physics, Chemistry and Pharmacy, University of Southern Denmark, DK-5230, Odense M, Denmark
[d] Department of Biology, Humboldt University Berlin, Invalidenstr. 43, D-10115, Berlin, Germany
[e] Institute for Chemistry, University of Potsdam, Karl-Liebknecht-Str. 24-25, D-14476, Potsdam, Germany
[f] Department of Developmental Biology, Washington University, St. Louis, MO, 63110, USA
[g] Taylor Family Institute for Innovative Psychiatric Research, St. Louis, Missouri, USA

## ARTICLE INFO

## ABSTRACT

Natamycin is an antifungal polyene macrolide that is used as a food preservative but also to treat fungal keratitis and other yeast infections. In contrast to other polyene antimycotics, natamycin does not form ion pores in the plasma membrane, but its mode of action is poorly understood. Using nuclear magnetic resonance (NMR) spectroscopy of deuterated sterols, we find that natamycin slows the mobility of ergosterol and cholesterol in liquid-ordered (Lo) membranes to a similar extent. This is supported by molecular dynamics (MD) simulations, which additionally reveal a strong impact of natamycin dimers on sterol dynamics and water permeability. Interference with sterol-dependent lipid packing is also reflected in a natamycin-mediated increase in membrane accessibility for dithionite, particularly in bilayers containing ergosterol. NMR experiments with deuterated sphingomyelin (SM) in sterol-containing membranes reveal that natamycin reduces phase separation and increases lipid exchange in bilayers with ergosterol. In ternary lipid mixtures containing monounsaturated phosphatidylcholine, saturated SM, and either ergosterol or cholesterol, natamycin interferes with phase separation into Lo and liquid-disordered (Ld) domains, as shown by NMR spectroscopy. Employing the intrinsic fluorescence of natamycin in ultraviolet-sensitive microscopy, we can visualize the binding of natamycin to giant unilamellar vesicles (GUVs) and find that it has the highest affinity for the Lo phase in GUVs containing ergosterol. Our results suggest that natamycin specifically interacts with the sterol-induced ordered phase, in which it disrupts lipid packing and increases solvent accessibility. This property is particularly pronounced in ergosterol containing membranes, which could underlie the selective antifungal activity of natamycin.

## 1. Introduction

Natamycin, also known as pimaricin, is an antifungal compound produced by certain types of bacteria. It is used as a food preservative to prevent the growth of mold and yeast on a variety of products, such as cheese and dried meats. Natamycin is effective against a wide range of fungi and has low toxicity to humans, making it a safer alternative to other antifungal compounds. It is commonly used in the food industry, as well as in the pharmaceutical and agricultural industries [1,2]. The mode of action of natamycin is not well understood. It is believed to work by interfering with the function of ergosterol, a critical component of the fungal cell membrane [3]. As a consequence, the activity of nutrient transporters is reduced causing impaired uptake of sugars and amino acids [4]. In a recent study, we demonstrated that natamycin interferes with ergosterol- dependent activity of the lysine transporter Lyp1 reconstituted into model membranes [5]. In contrast to other

---

polyenes, such as nystatin or amphotericin B (AmpB), natamycin does not form pores in lipid bilayers, such that a collapse of ion gradients across the plasma membrane (PM) is unlikely [3,6,7]. Natamycin may also have other mechanisms of action, such as inhibiting the fusion of yeast vacuoles or disruption of calcium homeostasis followed by loss of membrane potential, as shown for its action on leishmania parasites [8,9]. However, more research is needed to fully understand how natamycin interferes with fungal viability. Moreover, treatment of fungal infections with polyenes can cause side effects, such as nephrotoxicity, in the case of AmpB [10,11]. Thus, elucidating the mechanisms by which polyenes act selectively against fungal membranes is of high importance.

One aspect which deserves particular attention is the role of sterol-induced lipid phase behavior in polyene-membrane interactions. Both, mammalian cholesterol and yeast's ergosterol are able to order fatty acyl chains in fluid phospholipid membranes, which typically are at least monounsaturated and thereby above their chain melting temperature at room temperature, such as 1-palmitoyl-2-oleoyl-phosphatidylcholine (POPC) [12–14]. Similarly, the addition of either cholesterol or ergosterol to fully saturated PC, for example dipalmitoylphosphatidylcholine (DPPC) causes a disruption of the gel phase, this lipid forms at room temperature [15,16]. Above ca. 20–30 mol% of either sterol, the so-called liquid-ordered (Lo) phase is induced in both, POPC and DPPC membranes, which is enriched in sterols and phospholipids with fatty acyl chains primarily in trans configuration [14,17]. The sterol-induced Lo phase is characterized by intermediate lateral and fast axial diffusion of lipid constituents and is assumed to be highly relevant for biological membranes, especially the plasma membrane (PM) of yeast and mammalian cells [13,17,18]. Both sterols lower the lipid packing in gel-phase membranes consisting of phospho- or sphingolipids with saturated acyl chains, such as DPPC or N-palmitoyl-sphingomyelin (PSM) [19,20]. In mixtures of saturated and unsaturated phospholipids, cholesterol and ergosterol cause the co-existence of a sterol-rich Lo-phase with a fluid liquid-disordered (Ld) phase, but the precise phase boundaries and properties likely differ between both sterols [16,21,22].

For the pore-forming polyenes nystatin and AmpB, binding to membranes, self-association, and ion conductance have been shown to depend on the presence of sterols in the bilayer, often with more pronounced effects observed in ergosterol- compared to cholesterol-containing membranes [23–28]. Whether this difference is due to the specific interaction of these polyenes with ergosterol or due to specific properties of the ergosterol-induced membrane phase, is highly debated; while NMR studies with deuterated sterols show a preferred molecular interaction of AmpB with ergosterol, fluorescence and ion conductance studies with nystatin suggest a dominant role for the ergosterol-induced membrane phase in generating preferred affinity of the polyene to membranes containing the yeast sterol [23-26,29-31]. Whether sterol-induced lipid phase coexistence and domain properties also determine natamycin's membrane activity is not known. Using a variety of biophysical and biochemical methods, we showed recently, that natamycin inserted into model bilayers reduces the membrane condensing effect of both, cholesterol and ergosterol [5]. Natamycin was more efficient in 'fluidizing' membranes with ergosterol, and it interfered with the transport function of the lysine transporter Lyp1, whose activity strictly depends on ergosterol [5,32]. We also found evidence for the self-aggregation of natamycin in model membranes, and such aggregation was pronounced in membranes containing ergosterol [5]. Here, we employ a combination of NMR spectroscopy, molecular simulations, and fluorescence assays to show that natamycin interferes specifically with the ergosterol-induced ordered lipid phase in membranes. By making use of the intrinsic fluorescence of natamycin, we can directly visualize its interaction with this phase in model membranes. We also show that sterol-induced lipid packing is disturbed by natamycin resulting in increased accessibility to water and polar solutes. Finally, we discover that natamycin has a particularly strong effect on

interactions of sphingomyelin (SM) with ergosterol compared to cholesterol. Our results suggest that interaction and interference of natamycin with the sterol-rich Lo phase could underlie its antifungal activity in pathogenic yeast strains.

## 2. Materials and methods

### 2.1. Chemicals

Natamycin (#32417) and POPC (#850457P) were from MERCK KGaA. 1-palmitoyl- $d_{31}$–2–oleoyl-phosphatidylcholine (POPC-$d_{31}$), N-Palmitoyl- $d_{31}$-D-sphingomyelin (PSM- $d_{31}$), and the fluorescent 1-palmitoyl-2-(12-[N-(7-)-dodecanoyl]-phosphatidylcholine (NBD-PC) were purchased from Avanti Polar Lipids, Inc. (Alabaster, Al), while ergosterol, dehydroergosterol (DHE), steaoryl-D-sphingomelin (SSM) and N-Palmitoyl-D-sphingomyelin (PSM) were from MERCK, KGaA. Cholestatrienol (CTL) was synthesized as described (see protocol and references in [33]). The in carbon position 3 deuterium labelled sterols ergosterol-$d_1$ and cholesterol- $d_1$ were a generous gift from Micho Murata, Osaka University, Japan [29].

### 2.2. Liposome preparation and fluorescence spectroscopy

Large unilamellar vesicles (LUVs) were prepared by the extrusion method [34]. An aliquot of respective lipids and NBD-PC were dissolved in chloroform and dried in a rotating round-bottom flask under vacuum. For measuring the influence on dithionite-mediated fluorescence reduction (see below), natamycin (dissolved in methanol) was added to the lipids at this step of vesicle preparation. After the addition of a small volume of ethanol (final ethanol concentration was below 1% (v/v)) and HBS (HEPES buffered saline, 145 mM NaCl and 10 mM HEPES, pH 7.4), the mixture was vortexed and subjected to five freeze-thaw cycles. Subsequently, the lipid suspension was extruded 10 times through 0.1 μm polycarbonate filters at 40 °C (extruder from Lipex Biomembranes Inc., Vancouver, Canada; filters from Costar, Nucleopore, Tübingen, Germany). The reduction of NBD-PC upon the addition of dithionite was measured as described [35–37]. Briefly, LUVs were mixed in a fluorescence cuvette with HBS50 (HEPES buffered saline, 100 mM NaCl and 50 mM HEPES, pH 7.4) giving the following concentrations 33 μM lipid, 0.3 μM NBD-PC, and 3.3 μM natamycin. Subsequently, the NBD fluorescence was recorded at an emission of 540 nm ($\lambda_{ex}$ = 470 nm, slit width for excitation and emission, each 4 nm) by using an Aminco Bowman Series 2 spectrofluorometer (Urbana, IL) at 37 °C as a function of time. Thirty seconds after starting the measurement, sodium dithionite was added from a freshly prepared 1 M stock solution in 100 mM Tris (pH 10) giving a final dithionite concentration of 50 mM. After 300 s, Triton X-100 was added (final concentration of 0.5% (w/v)). By that, the bilayer structure was disrupted giving dithionite access to all NBD-PC resulting in a complete loss of fluorescence. As a control, vesicles with the same lipid compositions but without natamycin were also measured. The fluorescence values were normalized to those before the addition of dithionite and after the addition of Triton X-100 and fitted to a bi-exponential equation. From the fits, the rate constant ($k_p$) of the slow fluorescence decrease was determined. The $k_P$ values of the LUVs with natamycin were normalized to those of vesicles without natamycin and employed as a parameter for its influence on membrane integrity.

### 2.3. NMR spectroscopy

The respective molecules were mixed in the desired molar ratios in methanol/chloroform, and the solvent was evaporated. The samples were redissolved in cyclohexane and lyophilized overnight at high vacuum. After hydration with 40 wt% $H_2O$ for $^2H$ NMR (10 mM Hepes, 100 mM NaCl, pH 7.4), the samples were equilibrated by ten freeze-thaw cycles and gentle centrifugation. Static $^2H$ NMR spectra were measured on a Bruker (Bruker Biospin, Rheinstetten, Germany) Avance 750 for the

sample with the deuterated sterol or Bruker DRX300 (for samples containing chain deuterated POPC-$d_{31}$ or PSM- $d_{31}$) NMR spectrometer. The spectra were accumulated using the quadrupole echo pulse sequence [38]. The relaxation delay was 1 s, the delays between the 90° pulses (of ~3.1 μs) account for 50 μs.

### 2.4. Preparation and imaging of giant unilamellar vesicles (GUVs)

GUVs were prepared using the electro-swelling method [39] as described [40]. Briefly, lipid mixtures were prepared from stock solutions in chloroform. Subsequently, 100 nmol of POPC or of the domain forming lipid mixture POPC, SSM, and cholesterol or ergosterol (molar ratio 1:1:1) including 0.5 mol% of the liquid domain (Ld) marker NBD-PC were spotted onto custom-built titan chambers. For the preparation of GUVs with fluorescent sterols, ergosterol was replaced with DHE and cholesterol with CTL, respectively. These lipid mixtures were placed on a heater plate at 55 °C to facilitate solvent evaporation and subsequently put under high vacuum for at least 1 h in order to evaporate remaining traces of solvent. Lipid-coated slides were assembled using a spacer of Parafilm (Pechiney Plastic Packaging, Chicago, IL, USA) for insulation. The electro-swelling chamber was filled with 0.5 to 1 ml sucrose buffer (250 mM sucrose, 15 mM NaN3, osmolarity of 280 mOsm/kg) and sealed with plasticine. The plates were assembled for electroformation and an alternating electrical field of 10 Hz rising from 0.02 V to 1.1 V in the first 56 min was applied for 2.5 h to 3 h at 55 °C. To detach the vesicles from the slides the electrical field was changed to 4 Hz and 1.3 V and applied for 30 min.

UV-sensitive epifluorescence microscopy was done using a Leica DMIRBE microscope with a 63 × 1.4 NA oil immersion or 100 × 1.3 NA oil immersion Fluotar objective, respectively (Leica Lasertechnik GmbH). A Lambda SC smart shutter (Sutter Instrument Company) as illumination control. The microscope contains a 10x extra magnification lens in the emission light path, resulting in a final pixel size of 193 and 123 nm, for the 63x and 100x objectives, respectively. Natamycin was imaged using a specially designed filter cube obtained from Chroma Technology (Corp., Brattleboro, VA, USA) with a 335-nm (20-nm bandpass) excitation filter, 365-nm dichromatic mirror, and 405-nm (40-nm bandpass) emission filter. NBD-PC was imaged using a standard green filter set (470-nm (20- nm bandpass) excitation filter, 510-nm dichromatic mirror, and 537-nm (23-nm bandpass) emission filter). Between image acquisitions, the focus was adjusted to account for chromatic aberration between the UV channel on one hand, and the green and red channels on the other, as described [41]. The resulting images were postprocessed by deconvolution using the ImageJ plugin DeconvolutionLab [42]. The Richard-Lucy algorithm was used with 20 iterations, and a theoretical point spread function (PSF) was used for deconvolution and generated using the Diffraction PSF 3D plugin in ImageJ (https://imagej.net/plugins/diffraction-psf-3d). Settings were chosen according to the used channel and camera specifications.

### 2.5. Molecular simulations

Molecular dynamics (MD) trajectories of pure POPC membranes, POPC/cholesterol (70:30), and POPC/ergosterol (70:30) were obtained from our previous study [5]. These trajectories have a length of 500 ns. From the same work, also lipid membranes containing natamycin, either in monomeric (5 natamycin/leaflet), or dimeric form (3 natamycin dimers/leaflet) were used. The natamycin-containing membrane trajectories have a length of 1000 ns. We have reanalyzed these membranes concerning water transfers across the membrane, tilt angle distributions, rotational dynamics, and lateral diffusion of the sterols (see Results section). We tracked water transfers across the membranes with a simple counting technique [43]. The MD trajectories were unwrapped with the pbctools plugin in vmd [44]. The unwrapped trajectories were analyzed using the MDAnalysis python library by tracking the positions of water O atoms across time [45]. The membrane bilayers confine the z-positions

of the water molecules within "compartments," and water transfers by counting how many water molecules have entered into one of the periodic image compartments (above/below).

Tilt angles and positions of the sterol molecules were extracted using the MDAnalysis python library. [45] The sterol tilting angle was defined from the 'C3–C17' vector and the membrane bilayer normal. Tilt angle distributions were computed by generating histograms of the tilt angles. Autocorrelation functions of the sterols were computed using a Fast Fourier Transform (FFT). The lateral diffusion of sterols was estimated from the mean square displacement (MSD) of the sterols using FFTs. Before analysis, the net drift of the membranes was removed. Diffusion coefficients were estimated using linear regression on the MSDs. Error bars were estimated using bootstrapping.

## 3. Results and discussion

### 3.1. Natamycin slows the mobility of ergosterol and cholesterol in lipid bilayers to a similar extent

Our recent binding experiments with liposomes of varying acyl chain saturation indicate, that natamycin binds preferentially to lipid membranes containing ergosterol and saturated phospholipid species [5]. NOESY NMR measurements carried out in the same study could not reveal a stronger interaction of natamycin with ergosterol, indicating that the preferred binding of natamycin to ergosterol containing membranes is not the consequence of a higher affinity of the polyene to ergosterol compared to cholesterol. Instead, it could be the consequence of a preferred interaction of natamycin with a particular membrane phase or state induced by ergosterol more than by cholesterol in the lipid bilayer, like what has been suggested for nystatin [5,25,26,46]. However, the signal-to-noise ratio in these measurements was rather low, so we set out additional NMR experiments and molecular dynamics (MD) simulations to clarify this point.

For that, we made use of deuterated cholesterol and ergosterol analogs, as recently employed for AmpB [29]. Like what has been shown in this study for AmpB, we found that the quadrupolar splitting pattern of about 43 kHz visible in the absence of natamycin (Fig. 1A, B; black lines and arrows) is broadened and disappears in the presence of natamycin (Fig. 1A, B; red lines) for both deuterated sterols in POPC membranes. Since this splitting indicates a fast rotational averaging of the molecules, the spectra reflect an immobilization of both sterols in the presence of natamycin. The peak broadening observed in the NMR experiments is characteristic for sterol immobilization on the time scale of 10–100 μsec. That the effect is comparable for both sterols, suggests that natamycin affects the axial mobility of cholesterol and ergosterol on an intermediate time scale to a similar extent. In contrast, Matsumori and co-workers found for AmpB, using the same approach, ergosterol-specific interactions [29], which points to fundamental differences in the mode of action of both polyenes.

To follow up on our observations, we carried out MD simulations of POPC membranes containing natamycin and either cholesterol or ergosterol as recently described [5]. MD simulations access a shorter time scale, which is between about 1 ns to a few μs, depending on the total simulation run and the used sampling scheme.

For such simulations, the start conditions of natamycin organization in the lipid membrane has to be defined. While the molecular organization of natamycin in the bilayer is not certain, we assumed that it exists either in monomeric form or as aggregates, for which we found evidence by fluorescence spectroscopy in the same system [5]. The simplest aggregate form is a natamycin dimer, and we showed recently in MD simulations, that such dimers are more stable in membranes containing ergosterol compared to those with cholesterol, particularly for dimers in the antiparallel orientation [5]. Using this system, we analyzed the impact of natamycin on the tilt angle distribution of the sterols in the respective bilayers (Fig. 2A and B). For POPC/cholesterol membranes, the tilt angle distributions are almost identical between
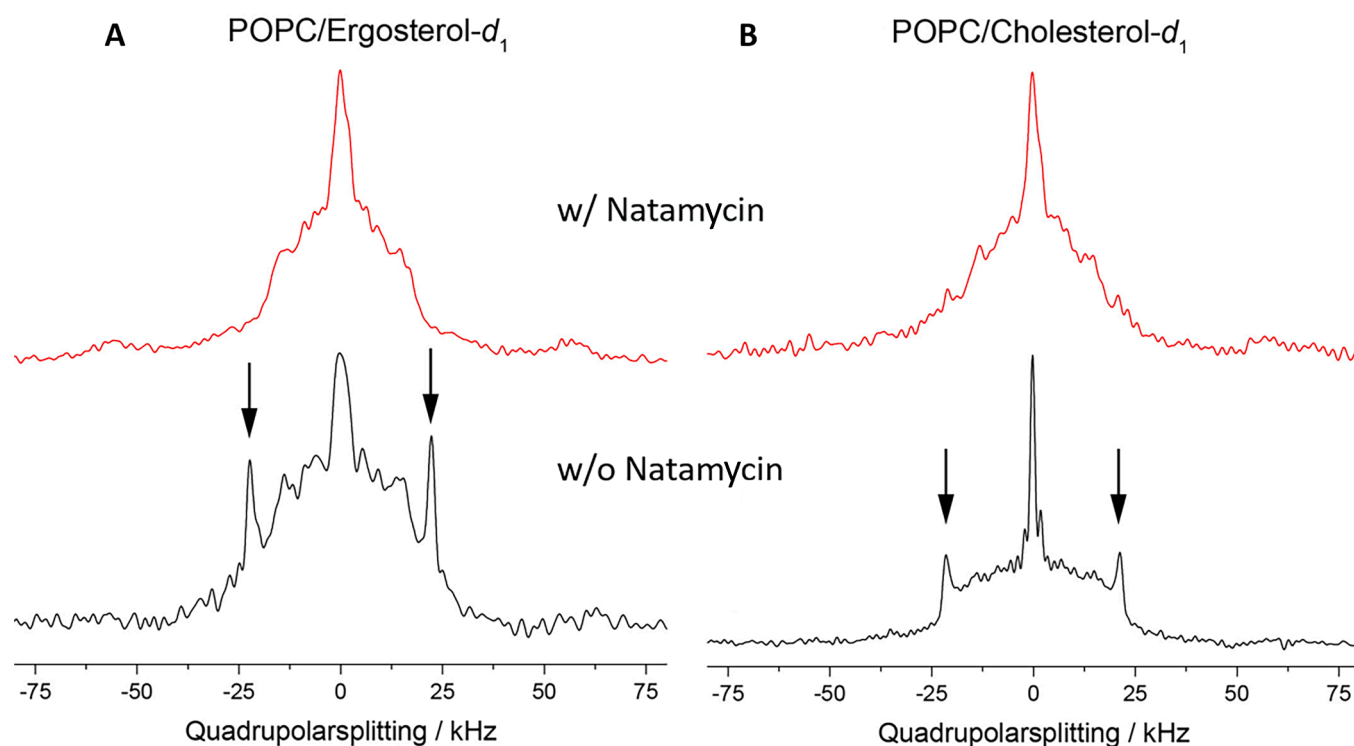
**Fig. 1.** NMR spectroscopy of deuterated cholesterol and ergosterol in model membranes.
$^2$H NMR spectra of ergosterol-$d_1$ (A) and cholesterol- $d_1$ (B) both deuterated in position carbon C3 each 20 mol% incorporated in POPC membranes in the presence (red spectra) or absence (black spectra) of 10 mol% natamycin. Natamycin slows the dynamics of both sterols as inferred from the absence of large quadrupolar splittings (arrows). The measurements were carried out at 25 °C.

pure and natamycin-containing membranes, with the first mode of the distribution (the mean tilt) at about 12°. For POPC/ergosterol membranes, natamycin has a minor effect on the tilt angle distributions, with a mean tilt at about 11°. Membranes with parallel natamycin dimers have slightly wider tilt angle distributions compared to bilayers containing antiparallel natamycin dimers. Overall, the tilt angle distributions are only weakly dependent on the incorporation of natamycin.

Next, we assessed the rotational dynamics of the sterols by calculating the autocorrelation function (ACF) of the long molecular axis and fitting it to a stretched exponential decay model (see Materials and Methods and Fig. 2C and D). This gives us the relaxation time of the tilt dynamics, either as time or as ensemble average. We find that the rotational dynamics of the sterol tilting angle is slowed upon the incorporation of natamycin in both POPC/cholesterol and POPC/ ergosterol membranes. The decay of the ACF is much more stretched than what can be described with a single exponential relaxation time with values of the stretching parameter at β=0.376–0.54 (Table 1). This stretched exponential decay with β < 1 is characteristic for molecular dynamics in lipid membranes due to heterogeneous fluctuations at different time scales [47]. The rotational slowdown due to the presence of natamycin is most significant in membranes containing parallel natamycin dimers, and it is slightly smaller in membranes containing cholesterol compared to those containing ergosterol. Parallel natamycin dimers are on average slightly closer to sterols than antiparallel dimers or natamycin monomers, as reflected in the RDF calculated for all membrane systems (Fig. S1).

Finally, we determined whether natamycin affects the lateral diffusion of both sterols (Table 2). We found that lateral diffusion of the sterols is generally slowed in membranes containing natamycin, particularly for membranes containing natamycin dimers. There is no significant difference between parallel and antiparallel dimers of natamycin, and both sterols are equally slowed in their lateral diffusion dynamics. Reduced lipid packing in the bilayer due to the presence of

natamycin also caused a slight increase in the crossing of water molecules across the bilayer, as calculated from the MD trajectories (Fig. S2). This was particularly pronounced for dimeric natamycin compared to natamycin monomers. Together, our results show that natamycin slows the dynamics of sterols in POPC membranes with a slightly stronger effect for bilayers with ergosterol compared to those with cholesterol. Natamycin in a dimeric state has a larger impact on sterol dynamics than natamycin monomers. This supports the conclusion from our previous work, which provided evidence for natamycin aggregation in membranes by fluorescence spectroscopy [5].

### 3.2. Natamycin interferes with sphingomyelin preferentially in ergosterol containing membranes

Since yeast cells contain large amounts of sphingolipids in their PM [48–50], we studied next the influence of natamycin on sphingomyelin (SM) containing membranes in the presence of sterols. $^2$H NMR spectra of deuterated PSM-$d_{31}$ mixed with 20 mol% of the respective sterol in the presence and absence of natamycin were measured. The spectra being measured at 37 °C to avoid the occurrence of gel phases are shown in Fig. 3. For PSM-$d_{31}$/ergosterol membranes in the absence of natamycin, two different sets of quadrupolar splittings can be observed in the spectra (highest quadrupolar splitting ∼ 35 kHz and ~55 kHz, respectively; see arrows). Similar spectra were previously observed for cholesterol containing membrane mixtures [51–53]. This indicates the presence of two phases with a different ergosterol content, which form domains large enough to avoid significant lipid exchange due to lipid diffusion in the time window of $^2$H NMR [51]. We interpret this - in line with observations in yeast, where highly ordered domains were observed before and classified - as ergosterol depleted and sphingolipid enriched domains [50]. Thus, the higher ordered domains with the higher quadrupolar splittings resemble ergosterol depleted domains, and we assign the lower splitting to an ergosterol enriched phase. In
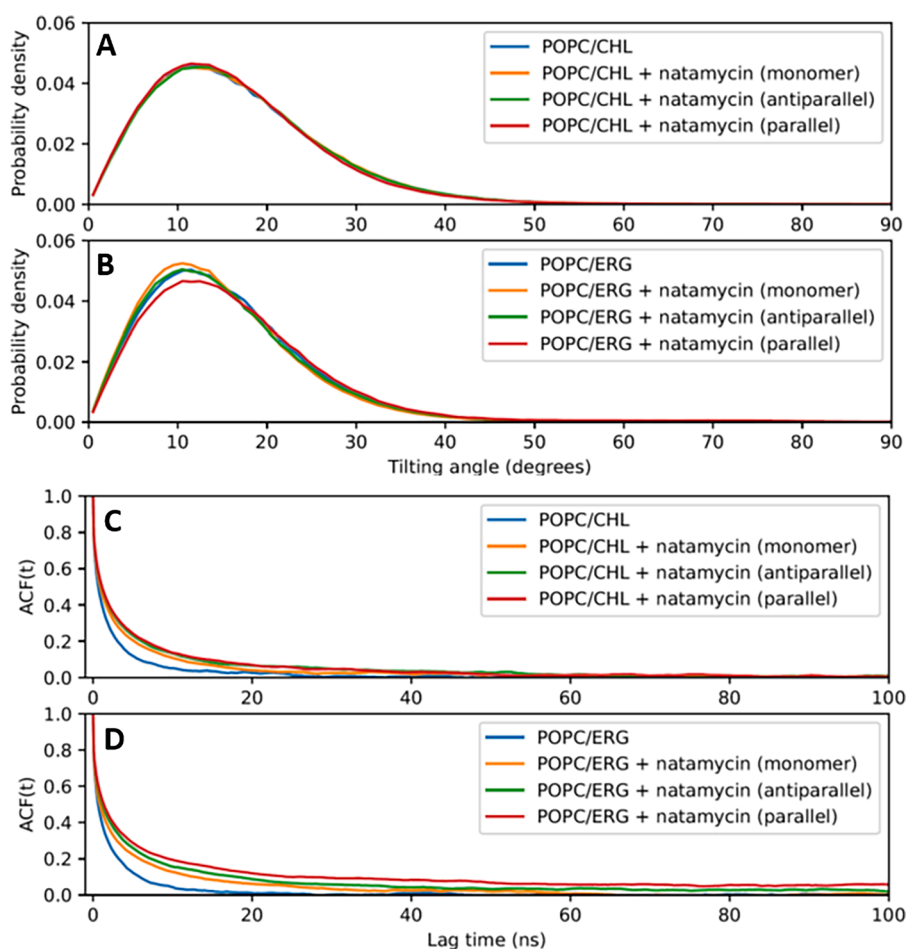
**Fig. 2.** MD simulations reveal slowed dynamics of sterols in the presence of natamycin.
Sterol tilt angle distributions for POPC/cholesterol (A) and POPC/ ergosterol membranes (B). Autocorrelation functions of the sterol tilt angles are plotted as a function of the lag time, ACF(t). The individually colored lines show data for pure POPC/cholesterol (C) or POPC/ergosterol membranes (D). The bilayers in all panels contained either no natamycin (blue lines), natamycin as monomers (orange lines), antiparallel dimers (green lines), or parallel dimers (red lines). See main text for further explanations.

**Table 1**
Autocorrelation analysis of sterol tilt dynamics in POPC membranes, Autocorrelation functions of the sterol tilt angles in membranes in the presence and absence of natamycin were fitted with a stretched exponential function, as described in Materials and methods. Both, the time-averaged and ensemble-averaged correlation times were determined.

| Membrane | Natamycin | $\tau_0$ | $\beta$ | RMSD | $R^2$ | $\bar{\tau}$ | $\langle\tau\rangle$ |
|---|---|---|---|---|---|---|---|
| POPC/CHL | – | 1.24 | 0.513 | 0.0074 | 0.996 | 2.37 | 6.69 |
| POPC/CHL | Monomers | 1.898 | 0.477 | 0.006096 | 0.9976 | 4.15 | 13.94 |
| POPC/CHL | Antiparallel | 2.204 | 0.446 | 0.008567 | 0.9954 | 5.56 | 22.14 |
| POPC/CHL | Parallel | 2.375 | 0.458 | 0.00453 | 0.9988 | 5.65 | 20.97 |
| POPC/ERG | – | 1.267 | 0.54 | 0.005825 | 0.9971 | 2.22 | 5.6 |
| POPC/ERG | Monomers | 1.974 | 0.441 | 0.003601 | 0.9991 | 5.11 | 20.97 |
| POPC/ERG | Antiparallel | 2.546 | 0.429 | 0.005019 | 0.9984 | 7.07 | 31.47 |
| POPC/ERG | Parallel | 2.986 | 0.376 | 0.012231 | 0.9896 | 11.87 | 77.15 |

**Table 2**
Lateral diffusion of cholesterol and ergosterol in POPC membranes, Lateral diffusion of cholesterol and ergosterol in membranes in the presence and absence of natamycin were calculated as described in Materials and methods.

| Sterol | Natamycin | Diffusion constant, D in cm²/s | Estimated error, std(D), in cm²/s |
|---|---|---|---|
| CHL | – | 2.19E-08 | 2.04E-09 |
| CHL | Monomers | 2.82E-08 | 1.95E-09 |
| CHL | Parallel dimers | 1.17E-08 | 1.22E-09 |
| CHL | Antiparallel dimers | 1.51E-08 | 1.45E-09 |
| ERG | – | 2.09E-08 | 1.73E-09 |
| ERG | Monomers | 1.34E-08 | 1.07E-09 |
| ERG | Parallel dimers | 1.13E-08 | 1.01E-09 |
| ERG | Antiparallel dimers | 1.35E-08 | 1.18E-09 |

contrast to this, in the presence of natamycin an averaged $^2$H NMR spectrum is observed, which indicates an enhanced and fast lipid exchange between the domains (Fig. 3). These results indicate that natamycin increases the mixing of ergosterol and SM, thereby causing domains to shrink. In the case of PSM-$d_{31}$/cholesterol membranes, a clear phase separation is not visible in the respective spectrum, and the difference to the spectra in the presence of natamycin is rather small, suggesting extensive lipid exchange in both cases.

Altogether, this means that for sphingomyelin/sterol membranes in the presence of ergosterol larger domains are formed than for cholesterol. This result confirms recent atomic force microscopy (AFM) studies, which found larger domains of POPC and egg yolk SM with a more pronounced height difference between phases in the presence of ergosterol compared to those with cholesterol [54]. We also find that the addition of natamycin to ergosterol/PSM membranes leads to smaller
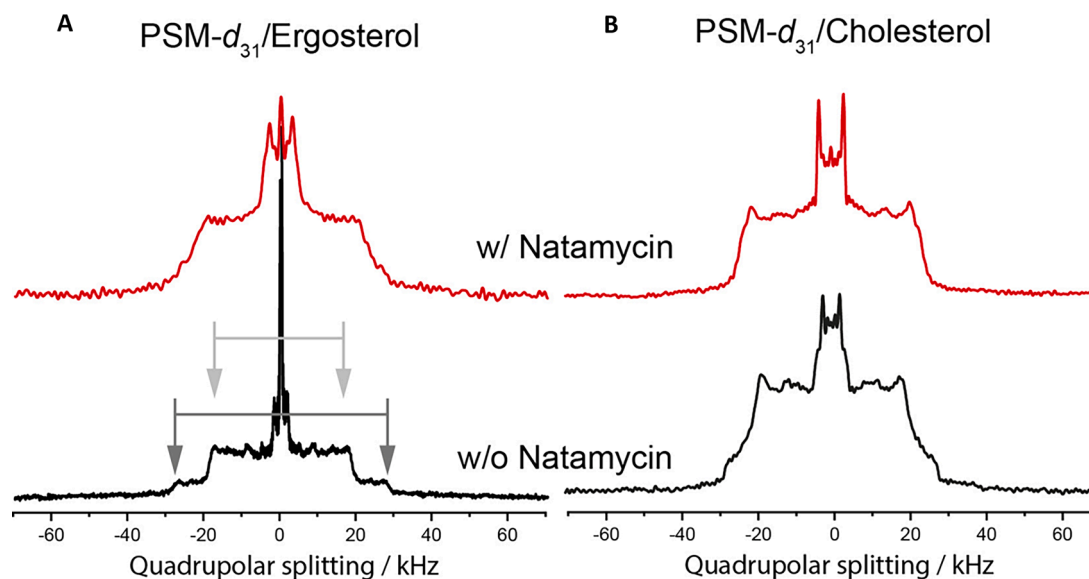
## A    PSM-$d_{31}$/Ergosterol

## B    PSM-$d_{31}$/Cholesterol

w/ Natamycin

w/o Natamycin

-60    -40    -20    0    20    40    60
Quadrupolar splitting / kHz

-60    -40    -20    0    20    40    60
Quadrupolar splitting / kHz

**Fig. 3.** Natamycin increases mixing of sphingolipids and ergosterol in model membranes.
$^2$H NMR spectra of PSM-$d_{31}$ in PSM/sterol (4/1) membranes (left for ergosterol, right for cholesterol) in the presence of natamycin (red) or for comparison in the absence (black) of 10 mol% natamycin. Without natamycin two different sets of quadrupolar splittings are observed in the spectrum of PSM-$d_{31}$/ergosterol (arrows), indicating larger membrane domains. In the presence of natamycin, these splittings are averaged, showing that significant lipid exchange takes now place on the timescale of $^2$H NMR experiments. The measurements were carried out at 37 °C.

domains with a reduced line tension and a faster lipid exchange [51,55]. This state seems comparable to the situation of PSM/cholesterol membrane already in the absence of natamycin. In conclusion, the results of these measurements reveal a unique structural organization of ergosterol and SM in lipid bilayers which is selectively perturbed by membrane-embedded natamycin. It is likely that such special interactions between ergosterol and sphingolipids also exist in the yeast PM, where they can be targeted by natamycin.

### 3.3. Natamycin alters the phase equilibrium of a ternary mixture of phospholipids and sterols

Since we find, that natamycin disturbs lipid packing in sterol-rich membranes, we asked next, how this polyene would impact the coexistence of Lo and Ld domains in more complex lipid membranes. To test that, we used NMR spectroscopy in ternary mixtures consisting of a lipid with low (POPC, $T_m$= - 2 °C), one with high melting temperature (PSM, $T_m$= 40 °C), and either cholesterol or ergosterol. The $^2$H NMR spectra of POPC-$d_{31}$ in POPC-$d_{31}$/PSM/Sterol (4/4/2) membrane with and without 10 mol% natamycin were recorded at intermediate temperature ($T$ = 20 °C) and are shown in Fig. 4. In the absence of natamycin and especially for the spectra of the POPC-$d_{31}$/PSM/cholesterol sample, both domains (Ld and Lo) are clearly visible since the different acyl chain order of the *sn*-1 chain of POPC in the two phases leads to a distinct quadrupolar splitting in the spectra. Additionally, to the dominating Ld phase with a well resolved set of smaller quadrupolar splittings, also the Lo phase is indicated by a second CD$_3$- splitting (i.e., of the deuterated methyl groups) in the middle of the spectrum (quadrupolar splitting ~5.4 kHz) and larger quadrupolar splittings above 20 kHz. The observation of these two phases in the $^2$H NMR spectra indicates that the high line tension between the domains leads to large domains due to coalescence to reduce the interface area and thereby the unfavorable line tension [51]. In contrast to the case of small domains, the quadrupolar splittings are not averaged out to a single component in the spectra, since the lipid exchange is slowed down in this case. Accordingly, phase separation observable in such spectra is reduced and finally vanished with increasing temperature, as the mixing entropy increasingly dominates over line tension between the phases.

In the numerical simulations of the $^2$H NMR spectra (Fig. 4) the

contributions of the Ld (green lines) and Lo phase (blue lines) add up to the respective spectra (red lines). At 20 °C about 30% of the spectra of POPC-$d_{31}$/PSM/cholesterol originated from the Lo phase. If cholesterol is replaced by ergosterol this amount is reduced to only ~10% probably due to the lower ordering effect of the yeast sterol [5]. It is known that the addition of small molecules can alter the domain structure and therefore may lead to changes in the respective spectra [51,56]. This is also the case for natamycin since the amount of the Lo phase in the spectra is significantly reduced for both membrane systems in the presence of the polyene. However, while in the presence of natamycin, no Lo phase could be observed in the ergosterol-containing membrane, the cholesterol-containing membrane still contained an amount of 5% of this phase. Additionally, also the quadrupolar splitting (and therefore the lipid chain order parameters) for the Ld phase are reduced in the presence of natamycin. This observation is consistent with the effect of natamycin in POPC-$d_{31}$/sterol membrane, where a disordering for the lipid chains was observed, which was more pronounced in the case of ergosterol [5]. These results indicate that membrane-embedded natamycin interferes with the ability of mammalian and yeast sterols to induce the Lo phase in ternary lipid mixtures. In the case of membranes with ergosterol, the Lo phase gets completely disrupted by membrane-embedded natamycin.

### 3.4. Natamycin decreases lipid packing in membranes and increases access for aqueous quenchers

While natamycin does not form classical pores for ions, in contrast to nystatin and AmpB [3,7,25,26,57], its membrane disturbing effect could potentially increase membrane access of (small) polar molecules. To test this notion, we employed a fluorescence assay based on quenching of the fluorescent phosphatidylcholine analogue NBD-PC by dithionite [58]. The permeation of dithionite is rather slow in pure lipid membranes, and its penetration kinetics can be used as a measure of lipid packing in the bilayer [59]. Fluorescence of NBD-tagged PC analogs can be efficiently reduced by dithionite upon contact of the fluorophore with the quencher, which results in biphasic fluorescence decays in case of dithionite permeation [59,60]. Likewise, we find that fluorescence quenching of NBD-PC in liposomes consists of a fast and a slow component (Fig. 5A). In the presence of natamycin, the second phase of
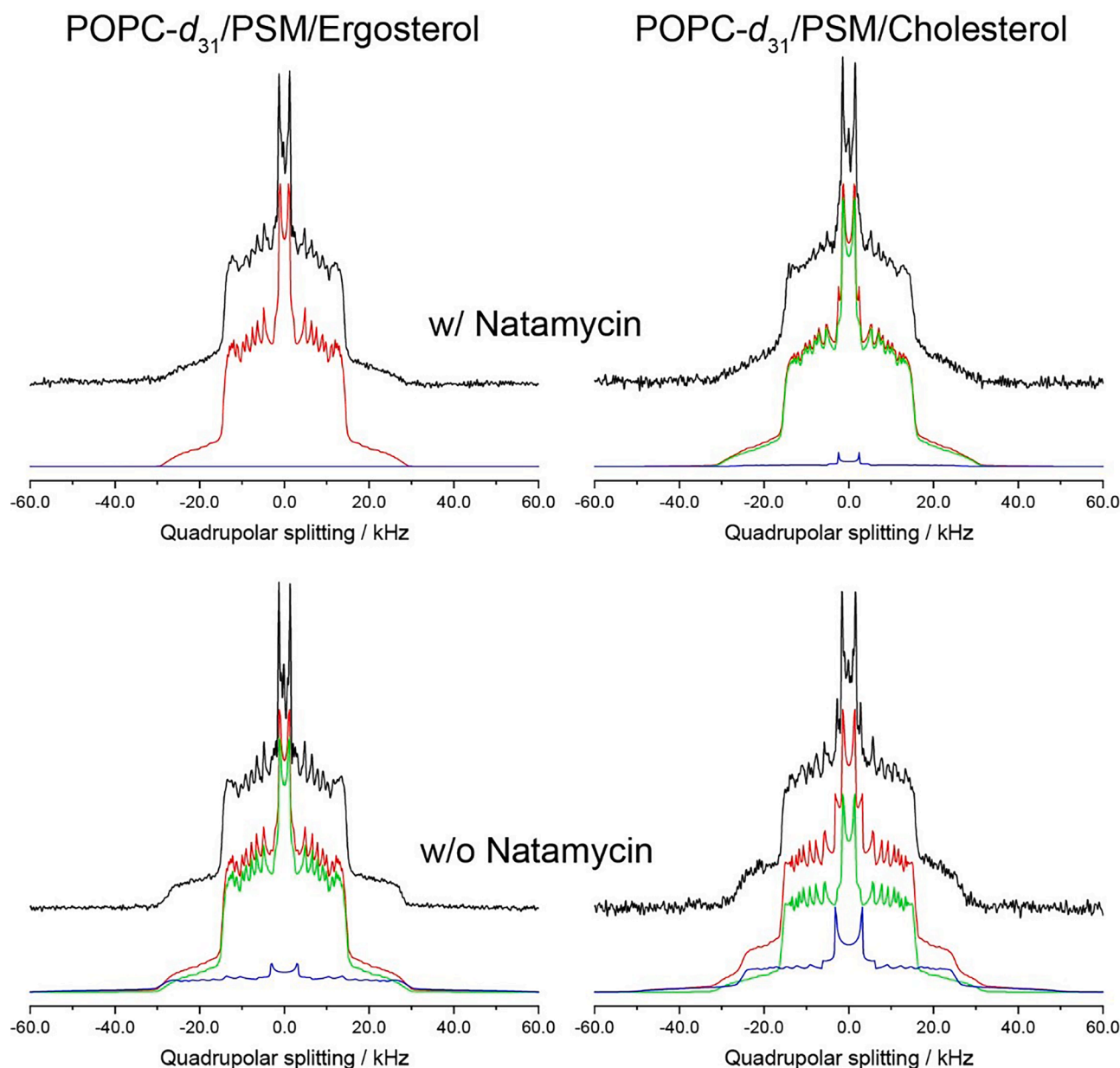
**Fig. 4.** Natamycin disturbs the phase behavior of ternary lipid membranes.
^{2}H NMR spectra (black) of POPC-$d_{31}$ in POPC-$d_{31}$/PSM/sterol (4/4/2) membranes (A, C for ergosterol, B, D for cholesterol) in the presence of natamycin (A and B) or for comparison in the absence of natamycin (C and D). The according numerical simulations of the spectra shown in red are the sum of the contributions of the Ld (green) and Lo (blue) phases. The spectra were measured at 20 °C. See main text for further explanations.

decaying NBD fluorescence is accelerated, suggesting that dithionite has increased access to a second pool of NBD-PC. We interpret this second pool as fluorescent lipid residing in the inner leaflet of the liposomes, which becomes accessible to dithionite in the presence of natamycin in the membrane. According to a recent study, the fluorescence curves should reflect most likely an accelerated dithionite movement across the membranes [61]. However, measuring accelerated reduction curves of NBD fluorescence can be principally also explained by an increased transbilayer movement of NBD-PC from the inner to the outer membrane leaflet, which is in a pure lipid membrane a very slow process, too [60,62]. In any case, the data reflects an increased permeation of a polar moiety across the bilayer indicating a reduced lipid packing in natamycin containing membranes. From the bi-exponential fits, the rate constant ($k_p$) of the second phase of fluorescence decrease of NBD-PC was determined (see Materials and methods). This shows accelerated quenching of NBD fluorescence by dithionite in the presence of

natamycin in ergosterol containing membranes (Fig. 5B). In contrast, only very little impact of natamycin was found in POPC/cholesterol membranes compared to liposomes consisting of pure POPC. These results suggest, that natamycin specifically impacts integrity and lipid packing in ergosterol containing membranes. This is in line with its pronounced effect on acyl chain ordering in bilayers containing ergosterol [5]. In membranes containing a mixture of POPC and SM in the presence of ergosterol or cholesterol lipid packing was increased, as indicated by the slowed access of dithionite to membrane embedded NBD-PC. This effect was much stronger for cholesterol- compared to ergosterol containing membranes, which is fully in line with the NMR experiments showing stronger interaction of SM with mammalian cholesterol compared to yeast's ergosterol. Interestingly, natamycin increases packing defects in membranes containing ergosterol and SM but not in those with cholesterol and SM (Fig. 5B). In the latter case, natamycin caused even a decrease in the already very low
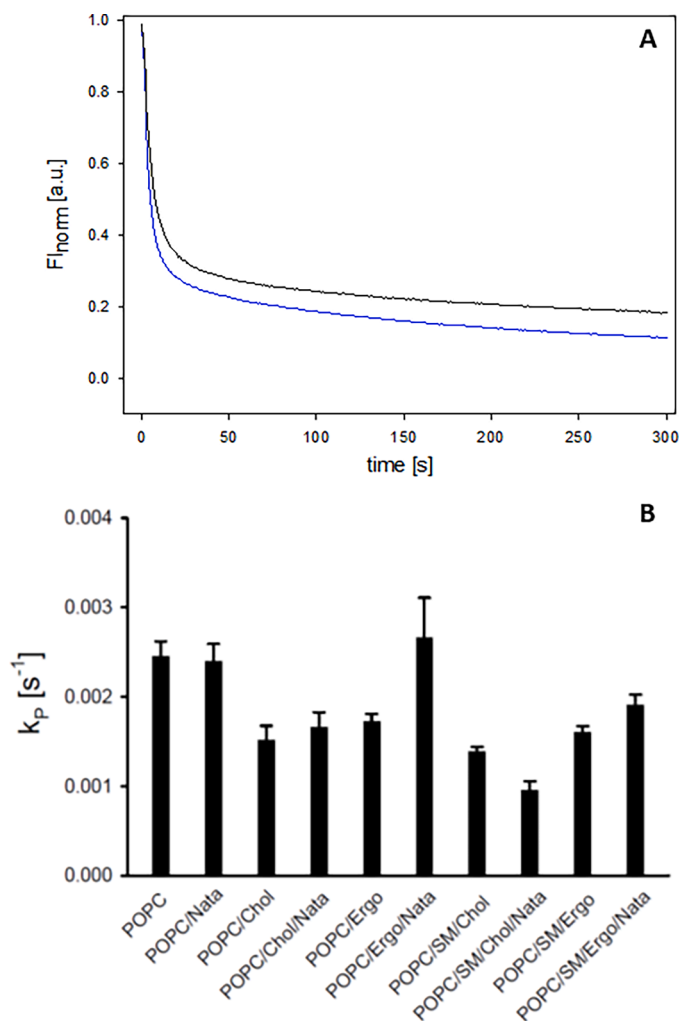
**Fig. 5.** Natamycin increases the accessibility to dithionite in a sterol-specific manner.

LUVs were prepared containing POPC, POPC/cholesterol or POPC/ergosterol (molar ratio 4:1), and POPC/SSM/ cholesterol or POPC/SSM/ ergosterol (molar ratio 4:1:1) without and with natamycin (molar ratio lipid/natamycin = 10). The reduction of NBD-PC's fluorescence upon the addition of dithionite was measured in POPC/ergosterol LUVs in the absence (black line) and in the presence (blue line) of natamycin as described in Materials and methods (A). This reveals a biphasic kinetics being characteristic for two differently accessible pools of NBD-PC. From the reduction curves, the rate constants ($k_P$) of dithionite access to the second pool were determined (B). The values with natamycin were normalized to those without natamycin. The mean values +/- SE are shown (1–2 independent samples each measured in triplicate).

dithionite-induced quenching of NBD-PC. These results suggest that natamycin preferentially interferes with SM-enriched domains, which are much more pronounced in ergosterol compared to cholesterol containing membranes because cholesterol can better interact and therefore mix with SM than ergosterol.

*3.5. Natamycin binds to the liquid-ordered phase, especially in ergosterol containing membranes*

All experiments described above were performed in membranes, in which natamycin was embedded during preparation. This strategy was chosen since our previous study showed that rapid membrane binding of the polyene is followed by a very slow intercalation step in model membranes [5]. To study the physiologically important initial interaction of natamycin with membranes, we made use of its intrinsic

fluorescence, which allows us to visualize natamycin binding to GUVs by UV-sensitive microscopy. Natamycin contains four conjugated double bonds giving rise to fluorescence in the near UV region of the spectrum, which can be detected using appropriate filter sets on a wide field microscope (Fig. 6A, B and Materials and methods). By adding natamycin to GUVs consisting of either POPC/PSM/ergosterol or POPC/PSM/-cholesterol, we can assess the binding preference of the polyene for different lipid phases. For the Ld phase, the green-fluorescent lipid analog NBD-PC was used, while the Lo phase contains no marker (Fig. 6C and D). We find that natamycin binds preferentially to the Lo phase in both types of GUVs, but this effect was much more pronounced for GUVs containing ergosterol compared to those containing cholesterol (Fig. 6C-F). Natamycin binds homogeneously along the entire Lo domain, ruling out that it gets enriched at phase boundaries, as has been suggested previously for nystatin [26,54]. Interestingly, in GUVs with internal membranes, which sometimes form during the preparation, natamycin is confined to the limiting membrane but has no access to the luminal vesicles. This was found for GUVs made with ergosterol (Fig. S3A) as well as for those with cholesterol (not shown). It shows that natamycin does not translocate across the bilayer and/or diffuses out of the inner leaflet in the time course of this experiment. The binding of natamycin to either the Ld or Lo phase can be quantified using line scans across GUVs, as illustrated in Fig. S3B, C and described in Materials and methods [63,64]. This analysis reveals a strong preference of natamycin for the Lo phase in GUVs with ergosterol compared to GUVs with cholesterol (Fig. 6D-F). This somehow surprising result could be due to different sterol enrichment in the Lo phase of either GUVs (i.e., different partitioning of ergosterol vs. cholesterol). To test this hypothesis, we made use of the intrinsically fluorescent analogs of ergosterol, DHE, and of cholesterol, CTL. Both sterol probes have identical fluorescence properties, very similar to natamycin, i.e., absorption and emission in the UV region of the spectrum [33]. Both probes are very similar to the respective natural sterols, DHE differs from ergosterol only by having one additional double bond in the ring system, while CTL has two more double bonds compared to cholesterol (Fig. 7A and B). The difference between both sterol probes is the same as between ergosterol and cholesterol, i.e., an extra double bond and methyl group in the alkyl chain for the yeast sterol. Using the same UV-optimized microscope setup as employed for imaging of natamycin, we assessed partitioning of the fluorescent sterols in GUVs made of either POPC/PSM/DHE or POPC/PSM/CTL, respectively. As a Ld marker, again NBD-PC was used.

We found that both sterols induce liquid-liquid phase separation and partition with high preference (i.e., close to 80%) into the Lo phase (Fig. 7C and D). There was no significant difference in phase preference between the ergosterol analogue DHE and the cholesterol analogue CTL, as shown by quantification of domain partitioning (Fig. 7E). These results make it unlikely that natamycin binds preferentially to the ergosterol-induced Lo phase because of higher availability of the sterol as binding partner compared to cholesterol containing GUVs. Instead, our results support the hypothesis that the Lo phase of ergosterol containing membranes has different properties than the Lo phase in membranes with cholesterol. This was already indicated in our previous study, in which we showed selective binding of natamycin to liposomes containing monounsaturated POPC or fully saturated DPPC and either ergosterol or cholesterol [5]. There, we showed that up to about 20 mol % sterol, natamycin binds preferentially to ergosterol containing membranes, while for higher sterol concentrations, it preferred cholesterol-containing membranes [5]. On the other hand, we showed in the same study that the ability to order fatty acyl chains in POPC is lower for ergosterol compared to cholesterol, which is in line with other studies, observing the same trend also for DPPC membranes [5,12,19, 65,66]. In particular, as we observed for natamycin binding [5], many studies showed a saturation effect of ergosterol on biophysical properties in POPC membranes, while POPC/cholesterol have a linear dependence of chain order, membrane stiffness, and dipole potential on sterol concentration to at least 40 mol% [12,67,68]. For GUVs with 33 mol%
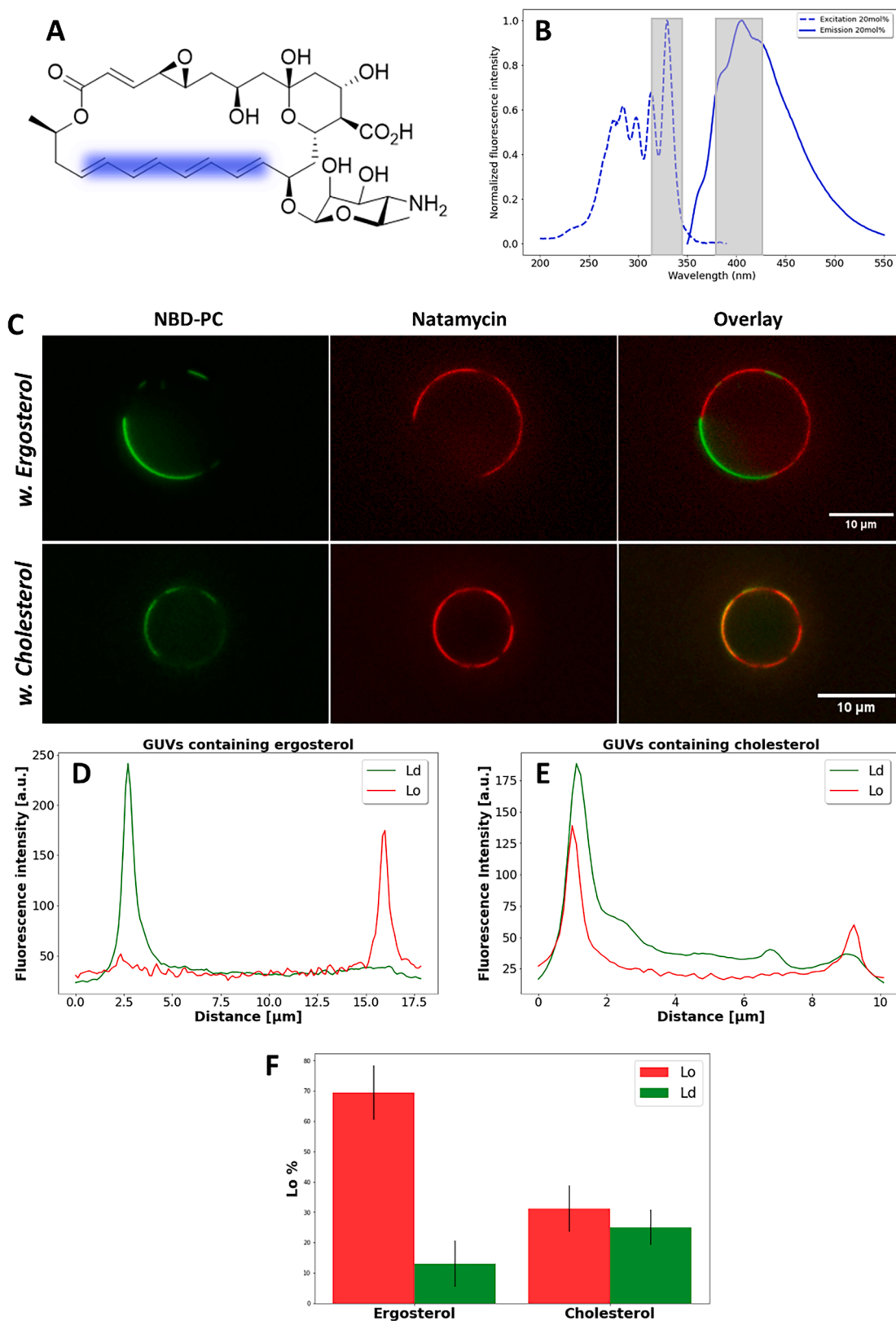
**Fig. 6.** Natamycin binds to the liquid-ordered phase in a sterol-dependent manner.
Structure of natamycin with conjugated double bonds (blue-shaded region) giving rise to its fluorescence are shown in A. Excitation (dashed blue line) and emission spectra (straight blue line) with overlayed bandpass of excitation and emission filter of the UV-optimized microscope used to image natamycin (B). GUVs consisting of POPS/SSM and either ergosterol or cholesterol are shown in C with natamycin in red and NBD-PC as a marker for the Ld phase in green. Line scans were performed over example vesicles indicating partitioning of natamycin (red) and NBD-PC (green) in GUVs containing either ergosterol (D) or cholesterol (E). From these scans, the percentage binding of natamycin to GUVs was quantified to the Lo phase (lacking NBD-PC, red) or Ld phase (containing NBD-PC, green) with either ergosterol or cholesterol (F). See main text for further explanations.
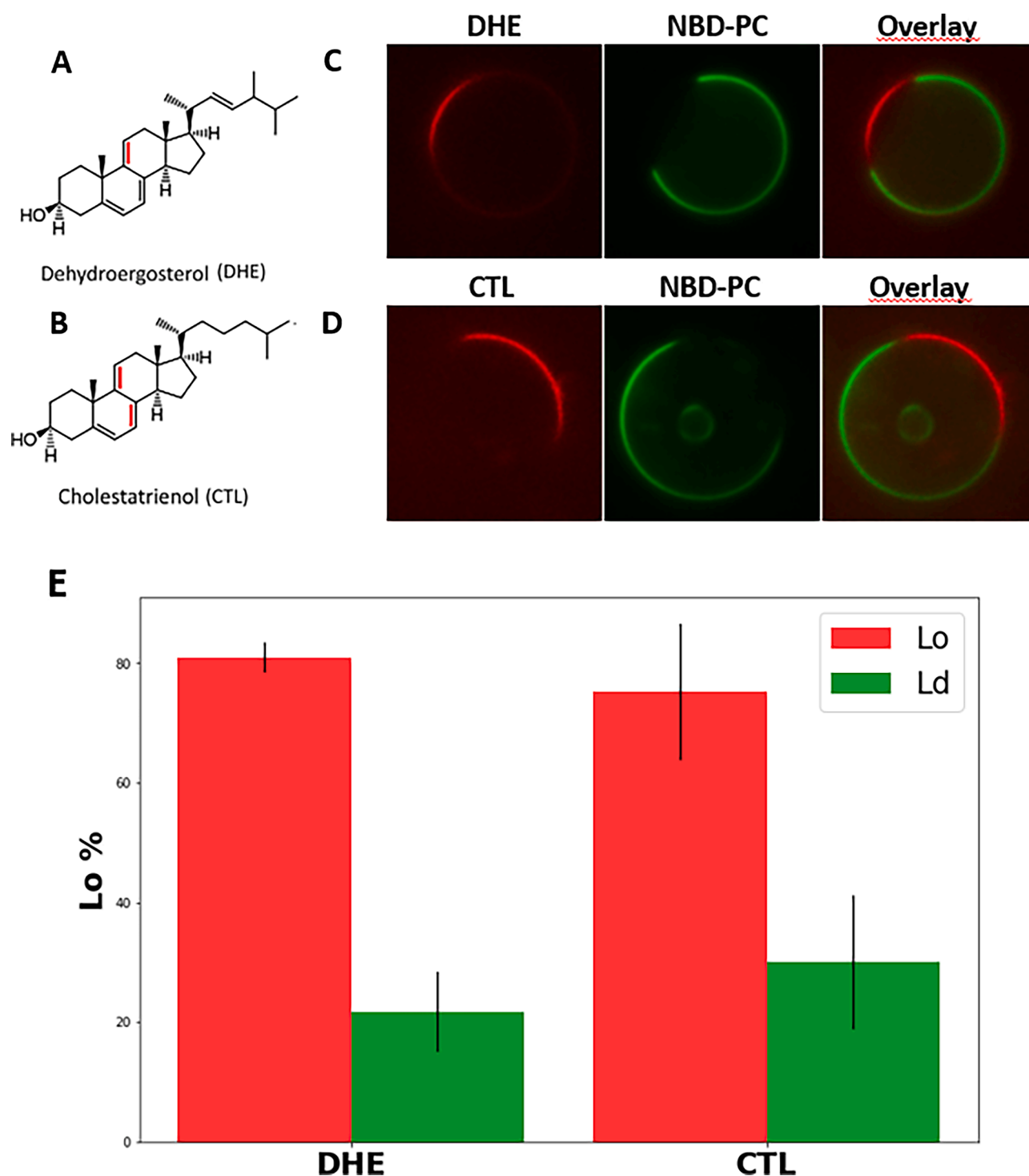
**Fig. 7.** Analogs of cholesterol and ergosterol become enriched in the liquid-ordered phase.

Structure of dehydroergosterol (DHE, A) and cholestatrienol (CTL, B), with differences to ergosterol and cholesterol indicated in red. GUVs consisting of POPC/SSM/DHE (1:1:1; C) and of POPC/SSM/CTL (1:1:1; D) with the respective sterol in red and NBD-PC in green, respectively, were examined microscopically. From the microscopic images, the percentage partitioning of DHE and CTL into the Lo phase (lacking NBD-PC, red) or Ld phase (containing NBD-PC, green) was quantified for GUVs with either DHE or CTL (E). See main text for further explanations.

sterol, a partitioning of 80:20 corresponds to 26.4 mol% sterol in the Lo phase and 6.6 mol% in the Ld phase, thus we expect based on our previous results, that binding of natamycin to the Lo phase in ternary lipid mixtures should be comparable for ergosterol compared to cholesterol containing GUVs. Based on these results, we conclude that the different properties of POPC/sterol membranes containing either ergosterol or cholesterol alone cannot explain the preferred interaction of natamycin with the Lo phase in GUVs with ergosterol. Thus, it is likely that the saturated SM plays a key role in the selective membrane interaction of the polyene. We speculate that the ergosterol-rich phase is particularly important to recruit natamycin to the membrane, but once in the bilayer, natamycin likely disrupts the Lo phase, thereby increasing lipid mixing and decreasing lipid packing.

## 4. Conclusions

In this study, we have combined NMR spectroscopy with MD simulations, fluorescence spectroscopy, and microscopy to uncover a preferred interaction of the ergosterol- induced Lo phase in model membranes with natamycin. Using deuterated sterols and MD simulations, we can show that natamycin slows the mobility of ergosterol and cholesterol to a comparable extent, which rules out that specific sterol-polyene interactions cause the preferred membrane interaction of natamycin. Instead, we find that natamycin disrupts the Lo phase in model membranes causing increased accessibility of aqueous quenchers to the membrane interior. These effects are more pronounced in ergosterol-enriched Lo phases compared to those induced by cholesterol, pointing to specific sterol-phospholipid interactions as key determinant for polyene-membrane interactions. Evidence for the importance of sterol-specific lipid phases has been presented previously for nystatin, amphotericin, and natamycin [5,25,26,30,46,69]. Here, we make use of the intrinsic fluorescence of natamycin to directly observe its preferred binding to the Lo phase in GUVs containing ergosterol by UV-sensitive microscopy. Using intrinsically fluorescent analogues of ergosterol, DHE, and of cholesterol, CTL, we can rule out that natamycin's preference for the ergosterol-induced Lo phase is due to the enrichment of this sterol in the Lo phase. Instead, our results suggest that specific packing properties of saturated SM, POPC, and ergosterol are responsible for natamycin's binding preference. Since the yeast PM not only differs in its sterol but also its sphingolipid composition from mammalian cell membranes [48,49], we hypothesize that the antifungal activity of natamycin could be a consequence of its preferred interaction with yeast-specific sphingolipids and ergosterol. Future studies are warranted to test this hypothesis in intact yeast cells.

## Declaration of Competing Interest

The authors declare that they have no known competing financial interests or personal relationships that could have appeared to influence the work reported in this paper.

## Acknowledgements

## Supplementary materials

Supplementary material associated with this article can be found, in the online version, at doi:10.1016/j.bbadva.2023.100102.

## References

[1] M. Meena, P. Prajapati, C. Ravichandran, R. Sehrawat, Natamycin: a natural preservative for food applications-a review, Food Sci. Biotechnol. 30 (2021) 1481–1496.

[2] Z. Qi, Q. Kang, C. Jiang, M. Han, L. Bai, Engineered biosynthesis of pimaricin derivatives with improved antifungal activity and reduced cytotoxicity, Appl. Microbiol. Biotechnol. 99 (2015) 6745–6752.

[3] Y.M. te Welscher, H.H. ten Napel, M.M. Balague, C.M. Souza, H. Riezman, B. de Kruijff, E. Breukink, Natamycin blocks fungal growth by binding specifically to ergosterol without permeabilizing the membrane, J. Biol. Chem. 283 (2008) 6393–6401.

[4] Y.M. te Welscher, M.R. van Leeuwen, B. de Kruijff, J. Dijksterhuis, E. Breukink, Polyene antibiotic that inhibits membrane transport proteins, Proc. Natl. Acad. Sci. USA 109 (2012) 11156–11159.

[5] M. Szomek, P. Reinholdt, H.L. Walther, H.A. Scheidt, P. Muller, S. Obermaier, B. Poolman, J. Kongsted, D. Wustner, Natamycin sequesters ergosterol and

[6] K.C. Gray, D.S. Palacios, I. Dailey, M.M. Endo, B.E. Uno, B.C. Wilcock, M.D. Burke, Amphotericin primarily kills yeast by simply binding ergosterol, Proc. Natl. Acad. Sci. USA 109 (2012) 2234–2239.

[7] J. Hou, P.N. Daniels, M.D. Burke, Small molecule channels harness membrane potential to concentrate potassium in trk1Deltatrk2Delta Yeast, ACS Chem. Biol. 15 (2020) 1575–1580.

[8] Y.M. te Welscher, L. Jones, M.R. van Leeuwen, J. Dijksterhuis, B. de Kruijff, G. Eitzen, E. Breukink, Natamycin inhibits vacuole fusion at the priming phase via a specific interaction with ergosterol, Antimicrob. Agents Chemother. 54 (2010) 2618–2625.

[9] B.P. Awasthi, K. Mitra, In vitro leishmanicidal effects of the anti-fungal drug natamycin are mediated through disruption of calcium homeostasis and mitochondrial dysfunction, Apoptosis 23 (2018) 420–435.

[10] P. Wasko, R. Luchowski, K. Tutaj, W. Grudzinski, P. Adamkiewicz, W.I. Gruszecki, Toward understanding of toxic side effects of a polyene antibiotic amphotericin B: fluorescence spectroscopy reveals widespread formation of the specific supramolecular structures of the drug, Mol. Pharm. 9 (2012) 1511–1520.

[11] E. Grela, M. Piet, R. Luchowski, W. Grudzinski, R. Paduch, W.I. Gruszecki, Imaging of human cells exposed to an antifungal antibiotic amphotericin B reveals the mechanisms associated with the drug toxicity and cell defence, Sci. Rep. 8 (2018) 14067.

[12] Y.W. Hsueh, M.T. Chen, P.J. Patty, C. Code, J. Cheng, B.J. Frisken, M. Zuckermann, J. Thewalt, Ergosterol in POPC membranes: physical properties and comparison with structurally similar sterols, Biophys. J. 92 (2007) 1606–1615.

[13] A. Khmelinskaia, J.M.T. Marques, A.E.P. Bastos, C.A.C. Antunes, A. Bento-Oliveira, S. Scolari, G. Lobo, R. Malho, A. Herrmann, H.S. Marinho, R.F.M. de Almeida, Liquid-ordered phase formation by mammalian and yeast sterols: a common feature with organizational differences, Front. Cell Dev. Biol. 8 (2020) 337.

[14] J.H. Ipsen, G. Karlstrom, O.G. Mouritsen, H. Wennerstrom, M.J. Zuckermann, Phase equilibria in the phosphatidylcholine-cholesterol system, Biochim. Biophys. Acta 905 (1987) 162–172.

[15] K.J. Tierney, D.E. Block, M.L. Longo, Elasticity and phase behavior of DPPC membrane modulated by cholesterol, ergosterol, and ethanol, Biophys. J. 89 (2005) 2481–2493.

[16] T.T. Bui, K. Suga, T.L. Kuhl, H. Umakoshi, Melting-temperature-dependent interactions of ergosterol with unsaturated and saturated lipids in model membranes, Langmuir 35 (2019) 10640–10647.

[17] P.J. Quinn, C. Wolf, The liquid-ordered phase in membranes, Biochim. Biophys. Acta 1788 (2009) 33–46.

[18] G. Oradd, P.W. Westerman, G. Lindblom, Lateral diffusion coefficients of separate lipid species in a ternary raft-forming bilayer: a Pfg-NMR multinuclear study, Biophys. J. 89 (2005) 315–320.

[19] Y.W. Hsueh, K. Gilbert, C. Trandum, M. Zuckermann, J. Thewalt, The effect of ergosterol on dipalmitoylphosphatidylcholine bilayers: a deuterium NMR and calorimetric study, Biophys. J. 88 (2005) 1799–1808.

[20] G. Oradd, G. Lindblom, P.W. Westerman, Lateral diffusion of cholesterol and dimyristoylphosphatidylcholine in a lipid bilayer measured by pulsed field gradient NMR spectroscopy, Biophys. J. 83 (2002) 2702–2704.

[21] P.J. Quinn, Long N-acyl fatty acids on sphingolipids are responsible for miscibility with phospholipids to form liquid-ordered phase, Biochim. Biophys. Acta 1788 (2009) 2267–2276.

[22] T.T. Bui, K. Suga, H. Umakoshi, Ergosterol-Induced Ordered Phase in Ternary Lipid Mixture Systems of Unsaturated and Saturated Phospholipid Membranes, J. Phys. Chem. B 123 (2019) 6161–6168.

[23] L. Silva, A. Coutinho, A. Fedorov, M. Prieto, Competitive binding of cholesterol and ergosterol to the polyene antibiotic nystatin. A fluorescence study, Biophys. J. 90 (2006) 3625–3631.

[24] A. Coutinho, L. Silva, A. Fedorov, M. Prieto, Cholesterol and ergosterol influence nystatin surface aggregation: relation to pore formation, Biophys. J. 87 (2004) 3264–3276.

[25] K.S. Recamier, A. Hernandez-Gomez, J. Gonzalez-Damian, I. Ortega-Blake, Effect of membrane structure on the action of polyenes: I. Nystatin action in cholesterol- and ergosterol-containing membranes, J. Membr. Biol. 237 (2010) 31–40.

[26] J. Gonzalez-Damian, I. Ortega-Blake, Effect of membrane structure on the action of polyenes II: nystatin activity along the phase diagram of ergosterol- and cholesterol-containing POPC membranes, J. Membr. Biol. 237 (2010) 41–49.

[27] W. Grudzinski, J. Sagan, R. Welc, R. Luchowski, W.I. Gruszecki, Molecular organization, localization and orientation of antifungal antibiotic amphotericin B in a single lipid bilayer, Sci. Rep. 6 (2016) 32780.

[28] A. Neumann, M. Wieczor, J. Zielinska, M. Baginski, J. Czub, Membrane sterols modulate the binding mode of amphotericin b without affecting its affinity for a lipid bilayer, Langmuir 32 (2016) 3452–3461.

[29] N. Matsumori, K. Tahara, H. Yamamoto, A. Morooka, M. Doi, T. Oishi, M. Murata, Direct interaction between amphotericin B and ergosterol in lipid bilayers as revealed by 2H NMR spectroscopy, J. Am. Chem. Soc. 131 (2009) 11855–11860.

[30] A. Coutinho, M. Prieto, Self-association of the polyene antibiotic nystatin in dipalmitoylphosphatidylcholine vesicles: a time-resolved fluorescence study, Biophys. J. 69 (1995) 2541–2557.

[31] L. Silva, A. Coutinho, A. Fedorov, M. Prieto, Nystatin-induced lipid vesicles permeabilization is strongly dependent on sterol structure, Biochim. Biophys. Acta 1758 (2006) 452–459.

[32] J.S. van 't Klooster, T.Y. Cheng, H.R. Sikkema, A. Jeucken, D.B. Moody, B. Poolman, membrane lipid requirements of the lysine transporter LYP1 from saccharomyces cerevisiae, J. Mol. Biol. (2020).

interferes with substrate transport by the lysine transporter Lyp1 from yeast, Biochim. Biophys. Acta (2022), 184012.

[33] M. Modzel, F.W. Lund, D. Wüstner, Synthesis and live-cell imaging of fluorescent sterols for analysis of intracellular cholesterol transport., in: I.C. Gelissen, A.J. Brown (Eds.) Meth. Mol. Biol., Place Published, 2017, pp. 111–140.

[34] L.D. Mayer, M.J. Hope, P.R. Cullis, A.S. Janoff, Solute distributions and trapping efficiencies observed in freeze-thawed multilamellar vesicles, Biochim. Biophys. Acta 817 (1985) 193–196.

[35] I. Haralampiev, D.J. Alonso de Armiño, M. Luck, M. Fischer, T. Abel, D. Huster, S. Di Lella, H.A. Scheidt, P. Müller, Interaction of the small-molecule kinase inhibitors tofacitinib and lapatinib with membranes, Biochim. Biophys. Acta 1862 (2020), 183414.

[36] H.A. Scheidt, I. Haralampiev, S. Theisgen, A. Schirbel, S. Sbiera, D. Huster, M. Kroiss, P. Müller, The adrenal specific toxicant mitotane directly interacts with lipid membranes and alters membrane properties depending on lipid composition, Molec. Cell. Endocrin. 428 (2016) 68–81.

[37] I. Haralampiev, H.A. Scheidt, T. Abel, M. Luckner, A. Herrmann, D. Huster, P. Müller, The interaction of sorafenib and regorafenib with membranes is modulated by their lipid composition, Biochim. Biophys. Acta 1858 (2016) 2871–2881.

[38] M.A. Davies, H.F. Schuster, J.W. Brauner, R. Mendelsohn, Effects of cholesterol on conformational disorder in dipalmitoylphosphatidylcholine bilayers. A quantitative IR study of the depth dependence, Biochemistry 29 (1990) 4368–4373.

[39] M.I. Angelova, S. Soléau, P. Méléard, J.F. Fuaucon, P. Bothorel, Preparation of giant vesicles by external AC electric fields. Kinetics and applications, Prog. Colloid Polym. Sci. 89 (1992) 127–131.

[40] I. Haralampiev, M. Mertens, R. Schwarzer, A. Herrmann, R. Volkmer, P. Wessig, P. Müller, Recruitment of SH-containing peptides to lipid and biological membranes through the use of a palmitic acid functionalized with a Maleimide Group, Angew. Chem. 54 (2015) 323–326.

[41] D. Wüstner, N.J. Færgeman, Chromatic aberration correction and deconvolution for UV sensitive imaging of fluorescent sterols in cytoplasmic lipid droplets, Cytometry. Part A 73 (2008) 727–744.

[42] D. Sage, L. Donati, F. Soulez, D. Fortun, G. Schmit, A. Seitz, R. Guiet, C. Vonesch, M. Unser, DeconvolutionLab2: an open-source software for deconvolution microscopy, Methods 115 (2017) 28–41.

[43] R.M. Venable, A. Kramer, R.W. Pastor, Molecular dynamics simulations of membrane permeability, Chem. Rev. 119 (2019) 5954–5997.

[44] W. Humphrey, A. Dalke, K. Schulten, VMD: visual molecular dynamics, J. Mol. Graph 14 (1996) 33–38, 27-38.

[45] N. Michaud-Agrawal, E.J. Denning, T.B. Woolf, O. Beckstein, MDAnalysis: a toolkit for the analysis of molecular dynamics simulations, J. Comput. Chem. 32 (2011) 2319–2327.

[46] A.G. Dos Santos, J.T. Marques, A.C. Carreira, I.R. Castro, A.S. Viana, M.P. Mingeot-Leclercq, R.F.M. de Almeida, L.C. Silva, The molecular mechanism of Nystatin action is dependent on the membrane biophysical properties and lipid composition, Phys. Chem. Chem. Phys. 19 (2017) 30078–30088.

[47] E.G. Brandt, O. Edholm, Stretched exponential dynamics in lipid bilayer simulations, J. Chem. Phys. 133 (2010), 115101.

[48] C.S. Ejsing, J.L. Sampaio, V. Surendranath, E. Duchoslav, K. Ekroos, R.W. Klemm, K. Simons, A. Shevchenko, Global analysis of the yeast lipidome by quantitative shotgun mass spectrometry, Proc. Natl. Acad. Sci. USA 106 (2009) 2136–2141.

[49] C. Klose, C.S. Ejsing, A.J. Garcia-Saez, H.J. Kaiser, J.L. Sampaio, M.A. Surma, A. Shevchenko, P. Schwille, K. Simons, Yeast lipids can phase-separate into micrometer-scale membrane domains, J. Biol. Chem. 285 (2010) 30224–30232.

[50] F. Aresta-Branco, A.M. Cordeiro, H.S. Marinho, L. Cyrne, F. Antunes, R.F. de Almeida, Gel domains in the plasma membrane of Saccharomyces cerevisiae: highly ordered, ergosterol-free, and sphingolipid-enriched lipid rafts, J. Biol. Chem. 286 (2011) 5043–5054.

[51] O. Engberg, A. Bochicchio, A.F. Brandner, A. Gupta, S. Dey, R.A. Bockmann, S. Maiti, D. Huster, Serotonin alters the phase equilibrium of a ternary mixture of phospholipids and cholesterol, Front. Physiol. 11 (2020), 578868.

[52] S.L. Veatch, O. Soubias, S.L. Keller, K. Gawrisch, Critical fluctuations in domain-forming lipid mixtures, Proc. Natl. Acad. Sci. USA 104 (2007) 17650–17655.

[53] T. Bartels, R.S. Lankalapalli, R. Bittman, K. Beyer, M.F. Brown, Raftlike mixtures of sphingomyelin and cholesterol investigated by solid-state 2H NMR spectroscopy, J. Am. Chem. Soc. 130 (2008) 14521–14532.

[54] A. Galvan-Hernandez, N. Kobayashi, J. Hernandez-Cobos, A. Antillon, S. Nakabayashi, I. Ortega-Blake, Morphology and dynamics of domains in ergosterol or cholesterol containing membranes, Biochim. Biophys. Acta 1862 (2020), 183101.

[55] R.D. Usery, T.A. Enoki, S.P. Wickramasinghe, M.D. Weiner, W.C. Tsai, M.B. Kim, S. Wang, T.L. Torng, D.G. Ackerman, F.A. Heberle, J. Katsaras, G.W. Feigenson, Line tension controls liquid-disordered + liquid-ordered domain size transition in lipid Bilayers, Biophys. J. 112 (2017) 1431–1443.

[56] G. Musabivora, O. Engberg, A. Gupta, D.S. Roy, S. Maiti, D. Huster, Serotonergic drugs modulate the phase behavior of complex lipid bilayers, Biochimie 203 (2022) 40–50.

[57] S.Z. Jokhadar, B. Bozic, L. Kristanc, G. Gomiscek, Osmotic effects induced by pore-forming agent nystatin: from lipid vesicles to the cell, PLoS ONE (2016) 11.

[58] J.C. McIntyre, R.G. Sleight, Fluorescence assay for phospholipid membrane asymmetry, Biochemistry 30 (1991) 11819–11827.

[59] M. Langner, S.W. Hui, Dithionite penetration through phospholipid bilayers as a measure of defects in lipid molecular packing, Chem. Phys. Lipids 65 (1993) 23–30.

[60] D. Huster, P. Muller, K. Arnold, A. Herrmann, Dynamics of membrane penetration of the fluorescent 7-nitrobenz-2-oxa-1,3-diazol-4-yl (NBD) group attached to an acyl chain of phosphatidylcholine, Biophys. J. 80 (2001) 822–831.

[61] A. Olzynska, W. Kulig, H. Mikkolainen, T. Czerniak, P. Jurkiewicz, L. Cwiklik, T. Rog, M. Hof, P. Jungwirth, I. Vattulainen, Tail-oxidized cholesterol enhances membrane permeability for small solutes, Langmuir 36 (2020) 10438–10447.

[62] T. Pomorski, A. Herrmann, A. Zachowski, P.F. Devaux, P. Muller, Rapid determination of the transbilayer distribution of NBD-phospholipids in erythrocyte membranes with dithionite, Mol. Membr. Biol. 11 (1994) 39–44.

[63] E. Sezgin, I. Levental, M. Grzybek, G. Schwarzmann, V. Mueller, A. Honigmann, V. N. Belov, C. Eggeling, U. Coskun, K. Simons, P. Schwille, Partitioning, diffusion, and ligand binding of raft lipid analogs in model and cellular plasma membranes, Biochim. Biophys. Acta 1818 (2012) 1777–1784.

[64] E. Sezgin, F. Betul Can, F. Schneider, M.P. Clausen, S. Galiani, T.A. Stanly, A. Colaco, A. Hongimann, D. Wüstner, F. Platt, C. Eggeling, A comparative study on fluorescent cholesterol analogs as versatile cellular reporters, J. Lipid Res. 57 (2016) 299–309.

[65] W.C. Hung, M.T. Lee, H. Chung, Y.T. Sun, H. Chen, N.E. Charron, H.W. Huang, Comparative study of the condensing effects of ergosterol and cholesterol, Biophys. J. 110 (2016) 2026–2033.

[66] A. Alavizargar, F. Keller, R. Wedlich-Soldner, A. Heuer, Effect of cholesterol versus ergosterol on DPPC bilayer properties: insights from atomistic simulations, J. Phys. Chem. B 125 (2021) 7679–7690.

[67] J. Henriksen, A.C. Rowat, E. Brief, Y.W. Hsueh, J.L. Thewalt, M.J. Zuckermann, J. H. Ipsen, Universal behavior of membranes with sterols, Biophys. J. 90 (2006) 1639–1649.

[68] S. Haldar, R.K. Kanaparthi, A. Samanta, A. Chattopadhyay, Differential effect of cholesterol and its biosynthetic precursors on membrane dipole potential, Biophys. J. 102 (2012) 1561–1569.

[69] A. Zumbuehl, P. Stano, D. Heer, P. Walde, E.M. Carreira, Amphotericin B as a potential probe of the physical state of vesicle membranes, Org. Lett. 6 (2004) 3683–3686.